Original Article

Glycyrrhetinic acid: A potential drug for the treatment of COVID-19 cytokine storm

Huawei Li [a,b,1], Jia You [b,1], Xi Yang [a,1], Yuanfeng Wei [a], Lingnan Zheng [a], Yaqin Zhao [a], Ying Huang [c], Zhao Jin [d,*], Cheng Yi [a,*]

[a] Department of Medical Oncology, Cancer Center, West China Hospital, Sichuan University, No.37 Guoxue Lane, Chengdu 610041, China
[b] Department of Oncology, Hospital of Chengdu University of Traditional Chinese Medicine, Chengdu 610072, China
[c] West China School of Basic Medical Science and Forensic Medicine, Sichuan University, Chengdu 610044, China
[d] School of Basic Medicine, Chengdu University of Traditional Chinese Medicine, Chengdu 611137, China

ARTICLE INFO

ABSTRACT

Background: The cytokine storm (CS) triggered by coronavirus disease 2019 (COVID-19) has caused serious harm to health of humanity and huge economic burden to the world, and there is a lack of effective methods to treat this complication.

Purpose: In this research, we used network pharmacology and molecular docking to reveal the interaction mechanism in the glycyrrhetinic acid (GA) for the treatment of CS, and validated the effect of GA intervention CS by experiments.

Study design: First, we screened corresponding target of GA and CS from online databases, and obtained the action target genes through the Venn diagram. Then, protein-protein interaction (PPI) network, Gene ontology (GO) analysis and Kyoto Encyclopedia of Genes and Genomes (KEGG) pathway enrichment of the action target genes were acquired by R language to predict its mechanism. Next, molecular docking was performed on core targets. Finally, experiments in which GA intervened in lipopolysaccharide (LPS)-induced CS were implemented.

Results: 84 action target genes were obtained from online database. The PPI network of target genes showed that TNF, IL6, MAPK3, PTGS2, ESR1 and PPARG were considered as the core genes. The results of GO and KEGG showed that action target genes were closely related to inflammatory and immune related signaling pathways, such as TNF signaling pathway, IL-17 signaling pathway, Human cytomegalovirus infection, PPAR signaling pathway and so on. Molecule docking results prompted that GA had fine affinity with IL6 and TNF proteins. Finally, *in vivo* and *in vitro* experimental results showed that GA could significantly inhibit LPS-induced CS.

Conclusion: GA has a potential inhibitory effect on CS, which is worthy of further exploration.

Introduction

COVID-19 is a huge catastrophe that has infected more than 400 million people and killed more than 6 million by April 2022, and the number of infections and deaths is increasing daily (https://covid19.who.int/). Many of those who died from COVID-19 induced hyper-inflammation characteristic of cytokine storm (CS) and related acute respiratory distress syndrome (ARDS) (Cron et al., 2021). CS is an out-of-control systemic inflammation disease induced by an overload of cytokines that led to multi-organ failure and even death (Behrens and Koretzky, 2017; Yongzhi, 2021). It is considered to be the main cause of severe COVID-19 patients. In general, the diseases are progressively aggravated as cytokine levels increase in COVID-19 patients (Pedersen and Ho, 2020). For example, patients who required admission to the ICU have significantly elevated levels of IL-6, TNF-α, IL-10, IL-2, etc. It is suggested the significance of CS in the pathogenesis and prognosis of

COVID-19. Therefore, the effective suppression of CS is crucial to prevent the deterioration of COVID-19 and to promote the treatment success rate.

Currently, the treatment of CS mainly includes glucocorticoids, blood purification therapy, biological agents and so on (Gao et al., 2021; Kim et al., 2021). Dexamethasone has been widely used in COVID-19 CS. In the RECOVERY trial, the result showed that dexamethasone could reduce mortality in patients who required mechanical ventilation and oxygen support. However, this was not evidence of a benefit for them with dexamethasone in milder cases (Horby et al., 2021). At the same time, the use of dexamethasone could reduce viral clearance and lead to exacerbations of disease (Andreakos et al., 2021). In addition, the side effects of glucocorticoids often significantly increase the difficulty of treatment, which is closely related to the poor prognosis (Oray et al., 2016). Blood purification therapy consists of plasma exchange, blood/plasma filtration, sorption, infusion, and continuous renal replacement therapy (CRRT) (Gao et al., 2021). These technologies also face challenges as they require expensive medical equipment and may cause machine-related damage. Biological agents as single target drugs, so far have not achieved good therapeutic results in the clinic. Therefore, the challenge of effectively treating COVID-19 CS remains enormous.

In China, Chinese herbal medicine is widely applied to address endemic and epidemic diseases. Among COVID-19 patients in Wuhan, there were no patients of mild and moderate symptoms developed severe symptoms when they received only Chinese herbal medicine treatment (Qiao et al., 2021). For most COVID-19 patients, a combination of Chinese and Western medicine can achieve a better overall response rate, a higher curative rate, a lower severe disease rate, a lower mortality rate, and a shorter hospitalization phase (Fu et al., 2021). Therefore, the application of Chinese herbal medicine in COVID-19 is worthy of in-depth exploration. According to the Chinese clinical strategy "Diagnosis and Treatment Protocol for Novel Coronavirus Pneumonia", licorice is one of the most used herbs in all herbal formulations that is recommended for treating COVID-19 (Wei, 2020). Glycyrrhizic acid (GLR) is a triterpenoid saponin primarily separated from the roots of the herb Glycyrrhiza glabra. It has antiviral and anti-inflammatory effects and might be used to relieve respiratory distress symptoms related with virus infections (Bailly and Vergoten, 2020; Sun et al., 2021). Consequently, it may be indicated to treat COVID-19 CS. Glycyrrhetinic acid (GA) is the main active metabolite of GLR which is formed by bacterial β-D-glucuronidase in the ileum and colon (Chrzanowski et al., 2021). The chemical structure of GA is similar to corticosteroids, so it has the functionality of glucocorticoid-like drugs, which include immune modulating and inflammation suppressing properties (Ding et al., 2020). Thus, GA may help to the control of CS.

Network pharmacology is a new discipline that is extensively utilized in the pharmaceutical research field. Through the network construction among drugs, diseases, proteins and pathways, we can better understand the interaction between drugs and diseases. Furthermore, it can help to improve clinical efficacy, reduce toxicity and elucidate multi-mechanisms of drugs (Lin et al., 2019). Consequently, we utilized network pharmacology, molecular docking and experimental verification to probe the effectiveness and potential mechanisms of GA for the treatment of CS.

In this study, the action targets of GA and CS were obtained and used to construct PPI network, GO and KEGG functional enrichment analysis. Meanwhile, the core targets of GA intervention CS were acquired through PPI network. Next, the interaction between GA and core genes were evaluated using molecular docking. In the meantime, LPS-induced CS model was applied to validate the inhibitory effect of GA on CS. This study provides a potential new drug for the treatment of CS with GA.

Materials and methods

Screening for GA and CS interacting target genes

The two-dimensional (2D) structure and SMILES of the GA were downloaded from PubChem database. And the SMILES was inputed in the Swiss Target Prediction database to got the target proteins with a probability > 0.1.

Target genes associated with CS were acquired from GeneCards, OMIM, and pharmgkb databases by using key words like "cytokine storm and cytokine release syndrome". Next, the Venn analysis tool was used to visualize the target genes of CS and GA, and this target gene cluster was considered as the action target genes associated with GA in CS.

Construction of PPI network and screening of core target genes

For the sake of explaining the mechanism of GA effect on CS, the String database was utilized to build the PPI network. The action target genes of CS and GA which were imported into the String database, and defined the gene source as "Homo sapiens". The confidence level was adjusted to 0.4 to acquire the relationship of protein interactions. At last, the result of the PPI network was exported to Cytoscape for visualization.

Then, through the network topology analysis plug-in CytoNCA to obtain core targets form the PPI network. The screening criteria for obtaining core targets are based on the following indicators: closeness centrality, betweenness centrality, degree centrality, eigenvector centrality, network centrality and local average connectivity. Meanwhile, the TSV file obtained from the String database were inputted into the R language software (V3.6.1) to calculate the number of adjacent nodes for each gene. According to the number of adjacent nodes to assessment the importance of genes.

GO function enrichment and KEGG pathway enrichment analysis

In the research, the R language org.hs.eg.db package was used to convert gene symbols to gene ID, and the R language DOSE, clusterProfiler, enrichplot, colorspace, stringi, BiocManager, ggplot2 package wereused to complete GO analysis, and to output the bubble diagram for the 3 modules of molecular function (MF), cellular composition (CC), and biological process (BP).

The R language dose, clusterprofiler, enrichplot, colorspace, stringi, ggplot2 and pathview packages were used to complete the KEGG enrichment visualization, and output the bubble diagram.

Molecular docking

Molecular docking was used to assess the likelihood of interaction and predict the binding mode of the ligand-proteins based on the knowledge of the three-dimensional (3D) structure (Zígolo et al., 2021). Therefore, the underlying mechanisms and interactions between GA and CS related target proteins may be revealed and forecasted by molecular docking.

SURFLEX dock mode in sybyl-x2.0 was utilized for molecular docking. The crystal structure of protease used for docking were retrieved from RCSB PDB database. The 2D molecular structure of GA was acquired from PubChem database, ChemBio3D Ultra 14.0 was used to minimize the energy of GA 2D structure to obtain the most stable molecular conformation. The Total-Score and Consensus Score scoring function were the Surflex-Dock molecular docking module, which were used to score the interaction between small molecules and targets.

Drug and reagent

Lipopolysaccharide (LPS) from *Escherichia coli* O111:B4 was obtained from Sigma-Aldrich (Shanghai China). Dexamethasone sodium

A

B
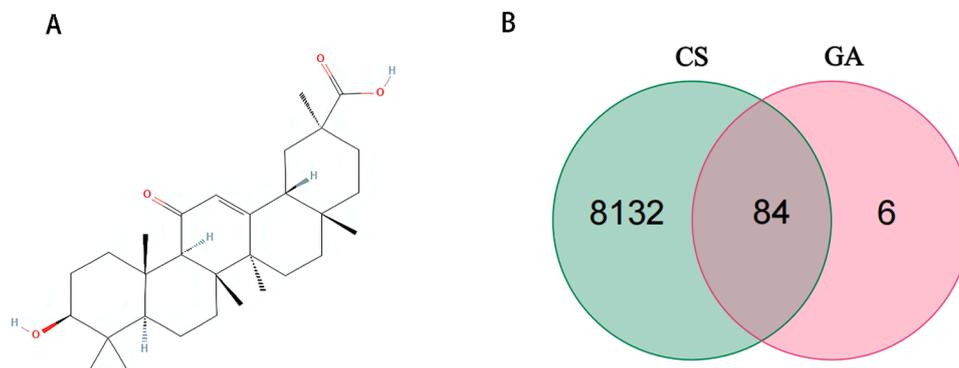
Fig. 1. The 2D structure of GA and target genes of GA acting on CS. (A) 2D structure of GA. (B) Venn diagram of GA and CS target genes.

phosphate injection (DEX) was purchased from Tianjin Jinyao Pharmaceutical Co., Ltd. GA (Cat#MB5206, meilunbio, China) was dissolved in dimethyl sulphoxide (DMSO) to obtain a stock concentration of 50 mg/kg and then diluted to the working concentrations *in vitro* experiments. *In vivo* experiments, GA was mixed with 0.9% normal saline (NS), and after ultrasound, a suspension was prepared for intragastric administration of mice. The rest of the supplies also include cell counting kit-8 (Cat#MA0218, meilunbio, China), mouse TNF-α ELISA kit (Cat#1217202, Dakewe, China), mouse IL-6 ELISA kit (Cat#1210602, Dakewe, China).

Cell counting kit-8 experiment

MH-S cells in a phase of exponential growth were seeded in 96-well plates at the density of 5×10^3/well overnight and then gave varying concentrations of GA. After 24 h, viability of cells was measured by CCK-8 assays.

In vitro experiments on CS

MH-S cells in the exponential growth phase were seeded at a density of 5×10^4/well into 48-well plates and incubated for 24 h. Then the cell received corresponding treatment measures according different experiment groups. In the experiment, it was divided into four groups and given the following interventions: control group (an equal volume-serum-containing medium), LPS group (an equal volume-serum-containing medium), DEX group (0.05μg/ml DEX), GA group (screening concentration of GA). After 24 h of cell culture, DEX group and GA group were added with drugs of corresponding concentrations respectively, and continued to be cultured in the cell incubator for 24 h. Then 100 ng/ml LPS was added in the LPS group, DEX group and GA group respectively, and the cell suspension was collected after 4 h. After centrifugation, the cell supernatant was collected, frozen at -80 °C, and stored pending cytokine assay.

In vivo experiments on CS

Eight-week-old male C57BL/6J mice weighing 24 – 26 g was randomly divided into NS group, LPS group, DEX group and GA groups with eight mice in each group. The GA group was administered 100 mg/kg GA suspension by gavage for 5 days, the DEX group was administered 1 mg/kg DEX by intraperitoneal injection for 3 days, the control group and LPS group were gavaged with equal volume of NS. 2 h after the last dose, the GA group, DEX group and LPS group were gave LPS (5 mg/kg) by intratracheal instillation, the NS group received NS alone without LPS treatment. 4 h after intratracheal instillation of LPS and bronchoalveolar lavage fluid (BALF) were collected from mice.

Enzyme-linked immunosorbent assay (ELISA)

The test samples were cell culture supernatant and mouse BALF. All operations were strictly in compliance with the instructions. After obtaining the OD value for each sample, the corresponding cytokine concentration in each sample was calculated based on the standard curve. GraphPad 9.0 software was used for data processing.

Immunohistochemistry

The expression of TNF-α and IL-6 in lung tissues was detected by immunohistochemistry. 5 μm lung sections were placed on slides and kept in an oven at 60 °C for 24 h. The slides were deparaffinized with xylene, dehydrated with various concentrations of alcohol, and then placed in retrieval solution and incubated in a microwave oven. The sections were then cooled, washed with washing buffer and incubated sequentially with primary antibody and biotin-labeled secondary antibody. Finally, sections were stained with DAB, stained with hematoxylin, dehydrated, washed with xylene, and fixed.

Histological study

Mice were sacrificed 24 h after LPS injection, then lung tissue was dissected and fixed with 4% paraformaldehyde. Next paraffin embedded, sectioned, and hematoxylin-eosin (HE) stained were used to prepare pathological sections.

Results

GA-related target genes in CS

2D structure (Fig. 1A) and SMILES of GA were obtained from PubChem. The chemical formula and molecular weight of GA are C30H46O4 and 470.7 g/M. Next, we obtained 90 target genes about GA from Swiss Target Prediction database. 8216 CS-related target genes were collected from the GeneCards, PharmGKB, and OMIM databases. 84 target genes were common genes in the two clusters of target genes, which was considered to be the action target gene of GA in the treatment of CS (Fig. 1B), specific information about the action target genes was presented in Table 1.

Construction of PPI network and acquisition of core target genes

The PPI network of action target genes were obtained from the String database. Then, visualization of PPI data was constructed by Cytoscape 9.0. For the sake of getting the core targets of GA, Cytoscape's CytoNCA plug-in was used. Based on the topological characteristics of network nodes, we selected the target points with betweenness centrality,

Table 1
The specific information about the action target genes.

No.	Uniprot ID	Gene Symbol	Gene Name
1	P01375	TNF	TNF-alpha
2	P05231	IL6	Interleukin-6
3	P35354	PTGS2	Cyclooxygenase-2
4	P24723	PRKCH	Protein kinase C eta
5	P14902	IDO1	Indoleamine 2,3-dioxygenase
6	Q07869	PPARA	Peroxisome proliferator-activated receptor alpha
7	Q03181	PPARD	Peroxisome proliferator-activated receptor delta
8	P80365	HSD11B2	11-beta-hydroxysteroid dehydrogenase 2
9	Q06124	PTPN11	Protein-tyrosine phosphatase 2C
10	P28845	HSD11B1	11-beta-hydroxysteroid dehydrogenase 1
11	O60218	AKR1B10	Aldo-keto reductase family 1 member B10
12	O14684	PTGES	Prostaglandin E synthase
13	P10275	AR	Androgen Receptor
14	P18031	PTPN1	Protein-tyrosine phosphatase 1B
15	P17706	PTPN2	T-cell protein-tyrosine phosphatase
16	O00748	CES2	Carboxylesterase 2
17	P35228	NOS2	Nitric oxide synthase, inducible
18	P11511	CYP19A1	Cytochrome P450 19A1
19	P08185	SERPINA6	Corticosteroid binding globulin
20	Q99720	SIGMAR1	Sigma opioid receptor
21	P04278	SHBG	Testis-specific androgen-binding protein
22	P05093	CYP17A1	Cytochrome P450 17A1
23	P06401	PGR	Progesterone receptor
24	P06276	BCHE	Butyrylcholinesterase
25	P04150	NR3C1	Glucocorticoid receptor
26	P56817	BACE1	Beta-secretase 1
27	P09917	ALOX5	Arachidonate 5-lipoxygenase
28	P30304	CDC25A	Dual specificity phosphatase Cdc25A
29	P35398	RORA	Nuclear receptor ROR-alpha
30	P27361	MAPK3	MAP kinase ERK1
31	Q01959	SLC6A3	Dopamine transporter
32	P29350	PTPN6	Protein-tyrosine phosphatase 1C
33	Q13133	NR1H3	LXR-alpha
34	P0DMS8	ADORA3	Adenosine A3 receptor
35	Q92731	ESR2	Estrogen receptor beta
36	P04054	PLA2G1B	Phospholipase A2 group 1B
37	P30305	CDC25B	Dual specificity phosphatase Cdc25B
38	P23141	CES1	Acyl coenzyme A:cholesterol acyltransferase
39	P10586	PTPRF	Receptor-type tyrosine-protein phosphatase F (LAR)
40	P24666	ACP1	Low molecular weight phosphotyrosine protein phosphatase
41	P31213	SRD5A2	Steroid 5-alpha-reductase 2
42	Q08499	PDE4D	Phosphodiesterase 4D
43	P07148	FABP1	Fatty acid-binding protein, liver
44	P08235	NR3C2	Mineralocorticoid receptor
45	P37231	PPARG	Peroxisome proliferator-activated receptor gamma
46	P03372	ESR1	Estrogen receptor alpha
47	O75469	NR1I2	Pregnane X receptor
48	P37058	HSD17B3	Estradiol 17-beta-dehydrogenase 3
49	O00767	SCD	Acyl-CoA desaturase
50	Q14994	NR1I3	Nuclear receptor subfamily 1 group I member 3 (by homology)
51	P11413	G6PD	Glucose-6-phosphate 1-dehydrogenase
52	Q16850	CYP51A1	Cytochrome P450 51 (by homology)
53	P37268	FDFT1	Squalene synthetase
54	P37059	HSD17B2	Estradiol 17-beta-dehydrogenase 2
55	P11387	TOP1	DNA topoisomerase I
56	P48147	PREP	Prolyl endopeptidase
57	P60033	CD81	CD81 antigen
58	P11388	TOP2A	DNA topoisomerase II alpha
59	P04035	HMGCR	HMG-CoA reductase
60	O00519	FAAH	Anandamide amidohydrolase
61	P15090	FABP4	Fatty acid binding protein adipocyte
62	P05413	FABP3	Fatty acid binding protein muscle
63	Q01469	FABP5	Fatty acid binding protein epidermal
64	P23219	PTGS1	Cyclooxygenase-1
65	O14746	TERT	Telomerase reverse transcriptase
66	P43116	PTGER2	Prostanoid EP2 receptor (by homology)
67	Q8TDU6	GPBAR1	G-protein coupled bile acid receptor 1

Table 1 (*continued*)

No.	Uniprot ID	Gene Symbol	Gene Name
68	P18405	SRD5A1	Steroid 5-alpha-reductase 1
69	P31645	SLC6A4	Serotonin transporter
70	P20292	ALOX5AP	5-lipoxygenase activating protein
71	Q9Y5Y4	PTGDR2	G protein-coupled receptor 44
72	P34995	PTGER1	Prostanoid EP1 receptor
73	P29317	EPHA2	Ephrin type-A receptor 2
74	P35408	PTGER4	Prostanoid EP4 receptor (by homology)
75	P52895	AKR1C2	Aldo-keto reductase family 1 member C2
76	Q04828	AKR1C1	Aldo-keto reductase family 1 member C1
77	P15104	GLUL	Glutamine synthetase
78	Q15722	LTB4R	Leukotriene B4 receptor 1
79	Q12908	SLC10A2	Ileal bile acid transporter
80	Q00987	MDM2	p53-binding protein Mdm-2
81	P08254	MMP3	Matrix metalloproteinase 3
82	P03956	MMP1	Matrix metalloproteinase 1
83	P08253	MMP2	Matrix metalloproteinase 2
84	O14842	FFAR1	Free fatty acid receptor 1

closeness centrality, degree centrality, eigenvector centrality, local average connectivity, and network centrality Values greater than the median in the network node as the core genes. Through two screenings (Fig. 2A), 9 core target were finally obtained, including TNF, IL6, MAPK3, NR3C1, PTGS2, PPARG, CYP19A1, ESR1, AR. These targets were considered the core targets of GA in the treatment of CS.

Meanwhile, the R language was used to obtain the bar graph of PPI core targets, which were arranged in descending order according to the number of adjacent nodes of the gene, as shown in the Fig. 2B. The number of adjacent nodes reflects the importance of genes in the network. The larger the number of adjacent nodes were, the greater the importance of the gene was. As indicated in Fig. 2B, TNF, IL6, PPARG, MAPK3, PTGS2, and ESR1 have the highest number of adjacent nodes and can be considered as the core genes in the PPI network. In Fig. 2, we can know that core genes obtained by this method basically consistent with those obtained by CytoNca plug-in.

GO enrichment analysis and KEGG pathway analysis

Depend on R language, GO analysis were performed on action target genes, which involved BP, CC and MF. According to the p value ($p <$ 0.05) , the items were filtered. Fig. 3 showed those top ten notably enriched BP, CC and MF categories.

In BP, the target genes were involvement in steroid metabolic process, steroid biosynthetic process, regulation of inflammatory response, cellular ketone metabolic process, fatty acid metabolic process, etc. It involved multiple inflammatory and metabolic processes.For CC, the targets were enriched in the nuclear envelope lumen, lipid droplet, membrane raf, etc; In MF, the target genes were extensively involved in the course of steroid dehydrogenase activity, steroid hormone receptor activity, steroid binding, icosanoid receptor activity, monocarboxylic acid binding, nuclear receptor activity, transcription coactivator binding, etc.

As shown in Fig. 4, the KEGG result included 22 pathways. These included TNF signaling pathway, IL-17 signaling pathway, PPAR signaling pathway, Steroid hormone biosynthesis, C−type lectin receptor signaling pathway, Human cytomegalovirus infection, and Arachidonic acid metabolism etc. These enriched pathways were closely related to the regulation of inflammation.

Molecular docking

A hyperinflammatory state with high concentrations of inflammatory cytokines has been demonstrated in COVID-19 patients. In addition, the core proteins such as TNF and IL6 were the most important nodes in the PPI network and KEGG pathway. Here, the molecular docking of GA with TNF, IL6, MAPK3, PTGS2, PPARG, and ESR1 were carried out, and

A

B
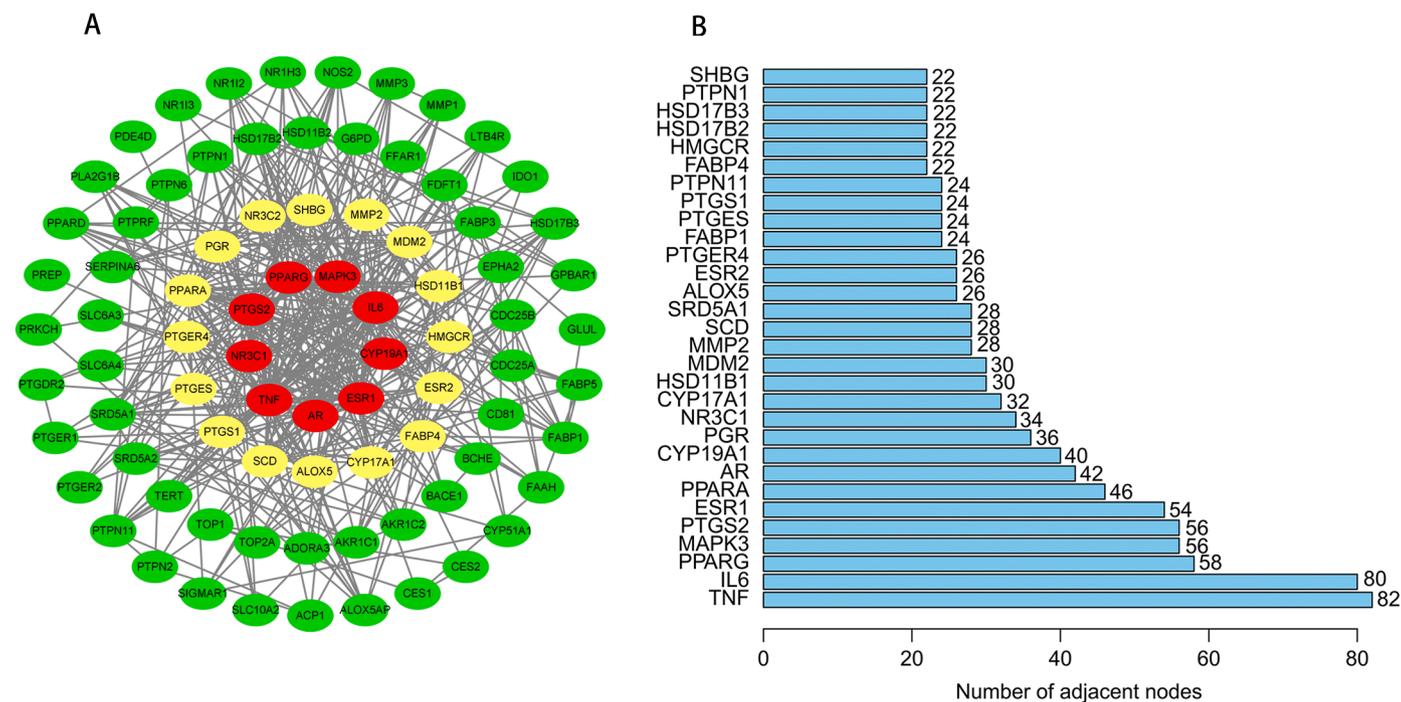
Fig. 2. Core targets of GA acting on CS. (A) Core Gene Screening via CytoNCA Plugin. (B) Core gene screening via R language.

the results showed that GA had fine affinity with these core targets (Fig. 5 and Table 2).

Generally, the higher the total score was, the more stable the binding was between the ligand and the target protein receptor. When the score is greater than 5, it indicates that the molecule has good binding activity with the target. C score mainly indicates the number of function scores that meet the requirements of molecular docking. The C score is 1~5, and the best C score is 5. The total score of GA with these proteins were greater than 3 and the C score were greater than 4, indicating that GA has good binding performance with the target, which can verify the binding activity between GA and the target to a certain extent.

GA significantly inhibit LPS-induced CS in MH-S cell

In order to obtain the optimal concentration of GA effect on MH-S cells, CCK-8 experiment was used. As indicated in the Fig. 6A, the cell viability of MH-S cells decreased gradually with the increase of GA concentration. When GA concentration was > 40 μg/ml, the cell viability of MH-S cells was significantly inhibited ($P < 0.0001$). When the concentration of GA was 0 – 5 μg/ml, it had no inhibit on the growth of MH-S cell. Consequently, 5 μg/ml was chosen as the dosing concentration for the cellular assay.

Based on the previous research, we used 100 ng/ml LPS to stimulate MH-S cells and successfully constructed a CS model. As shown in the Fig. 6B, LPS can significantly induce MH-S cells to secrete TNF-α, while GA can significantly inhibit TNF-α ($p < 0.05$). And GA has an anti-cytokine effect similar to that of DEX. Also, we performed IL-6 assays using this model. After LPS stimulation, IL-6 could be significantly elevated ($p < 0.001$). However, after GA intervention, there was no significant decrease in IL-6 (Fig. 6C).

GA significantly inhibit LPS-induced CS in vivo

As shown in Fig. 6E and F, following stimulation by LPS, TNF-α and IL-6 were remarkably increased in the LPS group($p < 0.01$ or $p < 0.0001$). After GA intervention, the expression of TNF-α and IL-6 could be significantly inhibited ($p < 0.05$ or $p < 0.05$). Meanwhile, in the LPS group, the total cell count in BALF was significantly elevated ($p < 0.01$).

After GA intervention, the total cell count could be significantly decreased ($p < 0.01$) (Fig. D). In terms of cytokines and total cell counts, it reflects that GA can significantly suppress inflammation.

Meanwhile, we used immunohistochemistry to assess the expression of TNF-α and IL-6 proteins in lung tissue. The proportion of positive regions of TNF-α and IL-6 was significantly higher in the LPS group compared with the NS group. In the DEX and GA groups, the proportion of positive regions was significantly reduced (Fig. 7).

In order to evaluate the therapeutic effect of GA on lung injury caused by LPS-induced CS, we observed histological changes in the lungs. The results showed that normal lung tissue structure and clear alveoli were observed in the NS group (Fig. 8A). Acute inflammation, congestion and edema were observed in the LPS group (Fig. 8B). Treatment in the DEX and GA groups significantly reduced structural damage to lung tissue compared to the LPS group (Fig. 8C, D).

Discussion

In the treatment of patients with COVID-19, a variety of traditional Chinese medicine are widely used including Lianhuaqingwen (LH) capsules, Qingfei Paidu decoction, etc. A multicenter, randomized controlled, and prospective trial showed that LH capsules could improve clinical symptoms of COVID-19. In patients using LH capsules, the median time to symptom recovery was significantly shorter than control group. The recovery time of fever, fatigue and cough was also significantly shorter. The efficacy of LH capsules in the treatment of COVID-19 was confirmed (Hu et al., 2021) LH capsules is composed of several Chinese herbal ingredients, among which licorice is one of the important drugs in LH capsules. Meanwhile, licorice is the most frequently used herb in Chinese formulas, known as 'National Venerable Master' (Guo et al., 2014). Licorice has a variety of components, the most important of them are GLR and its metabolite GA, which have been shown to have significant anti-inflammatory and antiviral effects.

The spike proteins is basic structure of coronavirus, which plays an important role in attachment, and into the host machinery. Spike protein consists of two subunits, S1 and S2 subunits. S1 binds to angiotensin-converting enzyme 2 (ACE2) through the receptor binding domain (RBD), in this manner, it mediates viral attachment to the cell surface
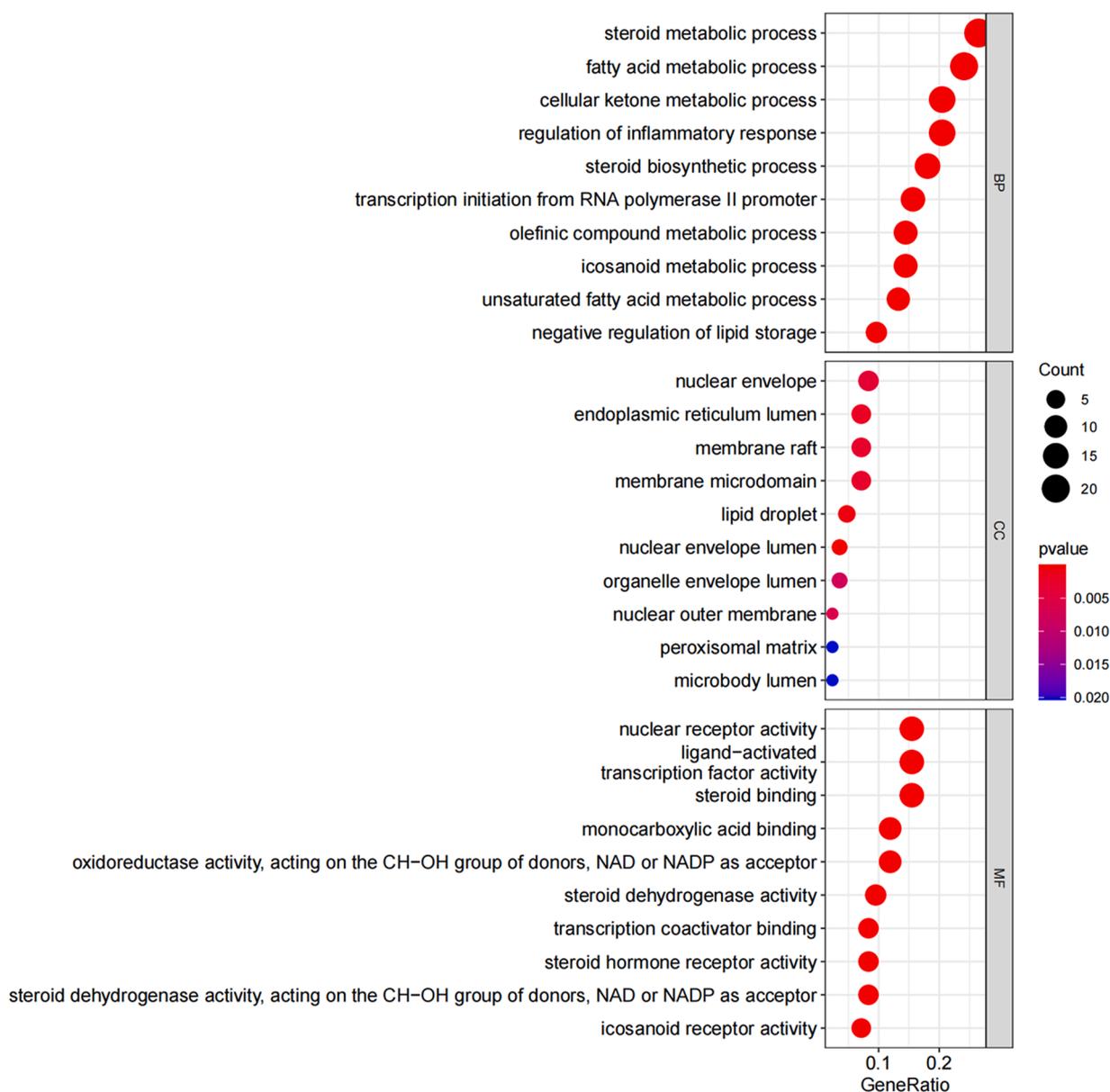
Fig. 3. The GO enrichment analysis of the action target genes.

and thus entry into the host. And ACE2 is a type 1 membrane protein that is a major target of coronavirus invasion (Ahmad et al., 2021). Shaopeng Yu et al. found that GLR has good activity in disrupting the interaction between SARS-CoV-2′s RBD and ACE2, thus exerting an inhibitory effect on SARS-CoV-2 (Yu et al., 2021). Meanwhile, a study showed that GLR could attenuate sepsis-induced acute lung injury (ALI), inhibit oxidative stress damage and apoptosis in lung tissue caused by ALI, and improve the survival rate of inflamed rats (Zhao et al., 2016). Yang Yi et al. screened 125 licorice compounds using molecular docking and found that GA showed significantly higher affinity to the RBD/ACE2 complex structure than GLR. Also, cellular experiments confirmed that GA inhibited SARS-CoV-2 virus in Vero E6 cells in a dose-dependent manner (Yi et al., 2022).

The above studies revealed significant antiviral and anti-inflammatory effects of GLR and the antiviral effects of GA, but few study on GA in the control of CS have been reported. Therefore, this research intends to reveal the effect of GA on CS and its potential mechanism through *in vivo* and *in vitro* experiments and network pharmacology.

We first screened the core targets of GA acting on CS, and the results

showed that TNF, IL6, MAPK3, PTGS2, PPARG, and ESR1 were the core targets. TNF as a vital cytokine, can evoke a number of intracellular signaling pathways, which include inflammation, apoptosis, cell survival and immunity (Blaser et al., 2016). The production of large amounts of TNF is closely related to the evolution of inflammatory illnesses, the likes of rheumatoid arthritis, inflammatory bowel disease and ARDS, which are often accompanied by high levels of TNF (Kalliolias and Ivashkiv, 2016). In the COVID-19 CS, TNF-α has a crucial role in the pathogenesis of CS and may contribute to escalation of disease severity (Kovalchuk et al., 2021). IL-6 is another crucial cytokine in the acute response of the host to infection. It can promote both inflammatory and immune responses, making it one of the key drug targets in auto-inflammatory and auto-immune illnesses (Tanaka et al., 2016). In COVID-19 patient, IL-6 is associated with patient viral load, severity, criticality and prognosis (Saghazadeh and Rezaei, 2020). The other core genes, like MAPK3 and PTGS2, also play an influential part in inflammation and viral infections (Grimes and Grimes, 2020; He et al., 2020).

The GO results showed that action target genes of GA were strong connection with inflammatory response and metabolic processes, including steroid metabolic process, regulation of inflammatory

Fig. 4. The KEGG pathway analysis of action target genes.

response, steroid biosynthetic process, steroid dehydrogenase activity, steroid binding, etc. The KEGG results focused on multiple inflammatory signaling pathways, it involved with IL-17 signaling pathway, TNF signaling pathway, PPAR signaling pathway, Steroid hormone biosynthesis, and so on. IL-17 signals via its relevant receptors and triggers downstream pathways, consisting of NF-κB, MAPKs and C/EBPs, to trigger the production of cytokines and chemokines (Shibabaw, 2020). TNF signaling pathway is widely involved in the systemic inflammatory response and is a pivotal inflammatory signaling pathway. After TNF binds to its receptor, it can induce activation of many genes, resulting in the production of large amounts of inflammatory cytokines. The TNF signaling pathway plays an important role in the regulation of immune cells. It was able to inhibit viral replication through IL-1 and IL-6 producing cells (Shawky et al., 2020). Steroid hormone biosynthesis is remarkably enriched in KEGG, and it perhaps is a druggable feature after

SARS-CoV-2 infection (Wu et al., 2021; Yang et al., 2020). Peroxisome proliferator-activated receptors (PPAR) belong to the nuclear hormone receptor family and are involved in a variety of pathophysiological processes *in vivo*, including cell differentiation, protein metabolism, lipid metabolism and inflammation. Ashmita Dey *et al.* revealed PPAR signaling pathway can play an important role for enhancing the infection after SARS-cov-2 intrusion via ACE2, suggesting the therapeutic targets in the COVID-19 (Dey et al., 2021). PPAR is distinguished into three subtypes: PPARα, PPARβ and PPARγ, in which PPARγ has a wide biological function on inflammatory regulation. Recent studies have noticed PPARγ agonists have therapeutic on CS in COVID-19 patients by regulating inflammation and immune response (Thomas et al., 2020; Vallée et al., 2021) .

COVID-19 CS as a process in which large amounts of inflammatory factors was released and inflammatory pathways was activated, which is
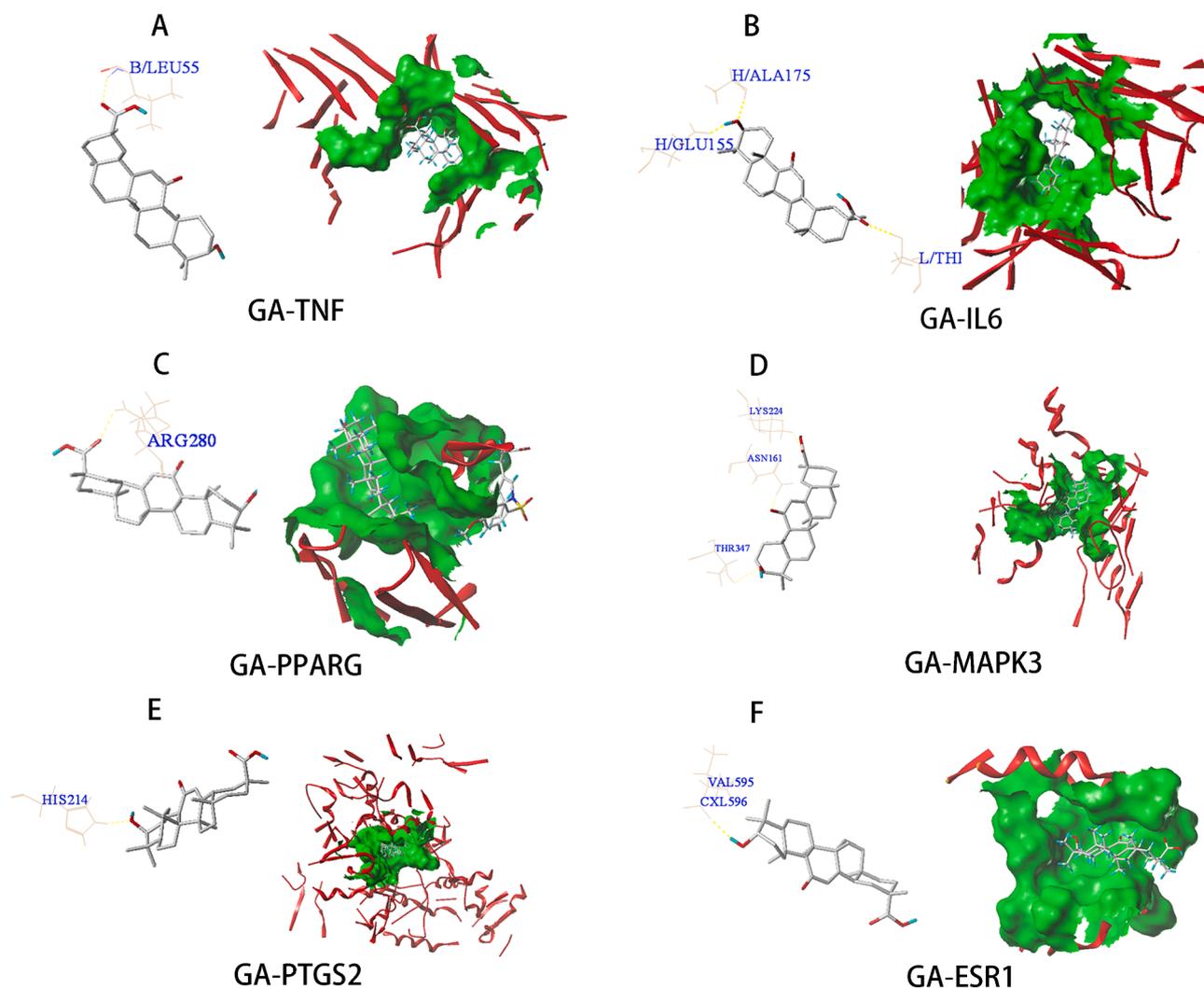
Fig. 5. Molecular docking of GA with target genes. (A–F)The molecular docking of GA with TNF, IL6, PPARG, MAPK3, PTGS2 and ESR1, respectively.

Table 2
Total score values & C score values of GA and core proteins.

Core Gene	PDB ID	Total Score	CSCORE
TNF	2AZ5	5.05	4
IL6	4CNI	6.04	4
PPARG	3ET3	3.57	4
MAPK3	4QTB	5.46	4
PTGS2	5IKQ	4.47	5
ESR1	4JC3	5.14	4

an important manifestation of the reaction between the virus and the body (Kawai and Akira, 2006). These inflammatory factors or pathways may be crucial routes for COVID-19 to induce CS and crucial routes for GA to inhibit cytokines.

Through network pharmacological analysis, it was confirmed that GA exerts anti-inflammatory effects through multiple targets and multiple pathways. In order to further explore its underlying mechanism, we conducted molecular docking studies. And the results showed that GA had good affinity with TNF, IL6, MAPK3, PTGS2, PPARG and ESR1. It is suggested that GA may exert anti-inflammatory effect through these targets.

LPS is a bacterial endotoxin that exists in gram-negative bacteria and is commonly used to construct inflammation models *in vivo* and *in vitro* (Li et al., 2021; Pooladanda et al., 2021). *In vitro*, we successfully constructed an LPS-induced CS model. After the intervention of GA, TNF-α can be significantly down-regulated. Although there was a trend for IL-6 to decrease in the GA group compared to the LPS group, there was no statistical difference. It was considered that due to the limited sample size, which could be expanded for the study at a later stage. *In vivo*, we constructed an animal CS model induced by LPS. In the LPS group, the TNF-α and IL-6 were significantly increased, suggesting that the LPS-induced CS animal model was successfully constructed. After the intervention of GA, TNF-α and IL-6 was decreased significantly. The results of immunohistochemistry also showed that GA significantly downregulated TNF-α and IL-6 proteins in lung tissue. The results of *in vivo* and *in vitro* experiments showed that GA can inhibit TNF-α and IL-6, which was consistent with the results of molecular docking. Meanwhile, the HE staining suggested that GA treatment reduced the inflammatory condition of the lungs and reduced neutrophil infiltration and alveolar congestion. The total cells in BALF were significantly reduced in the GA group, confirming the anti-inflammatory effect of GA from another perspective.

At present, there is no optimal treatment strategy for CS, which is a pressing medical problem. And the development of new drugs is a long process. Therefore, the repurposing of clinically drugs may be an effective strategy for the treatment of CS. In this research, the network pharmacology, molecular docking and experimental studies revealed that GA may exert anti-inflammatory effects through multiple targets and pathways. Consequently, GA may be a promising drug for CS.
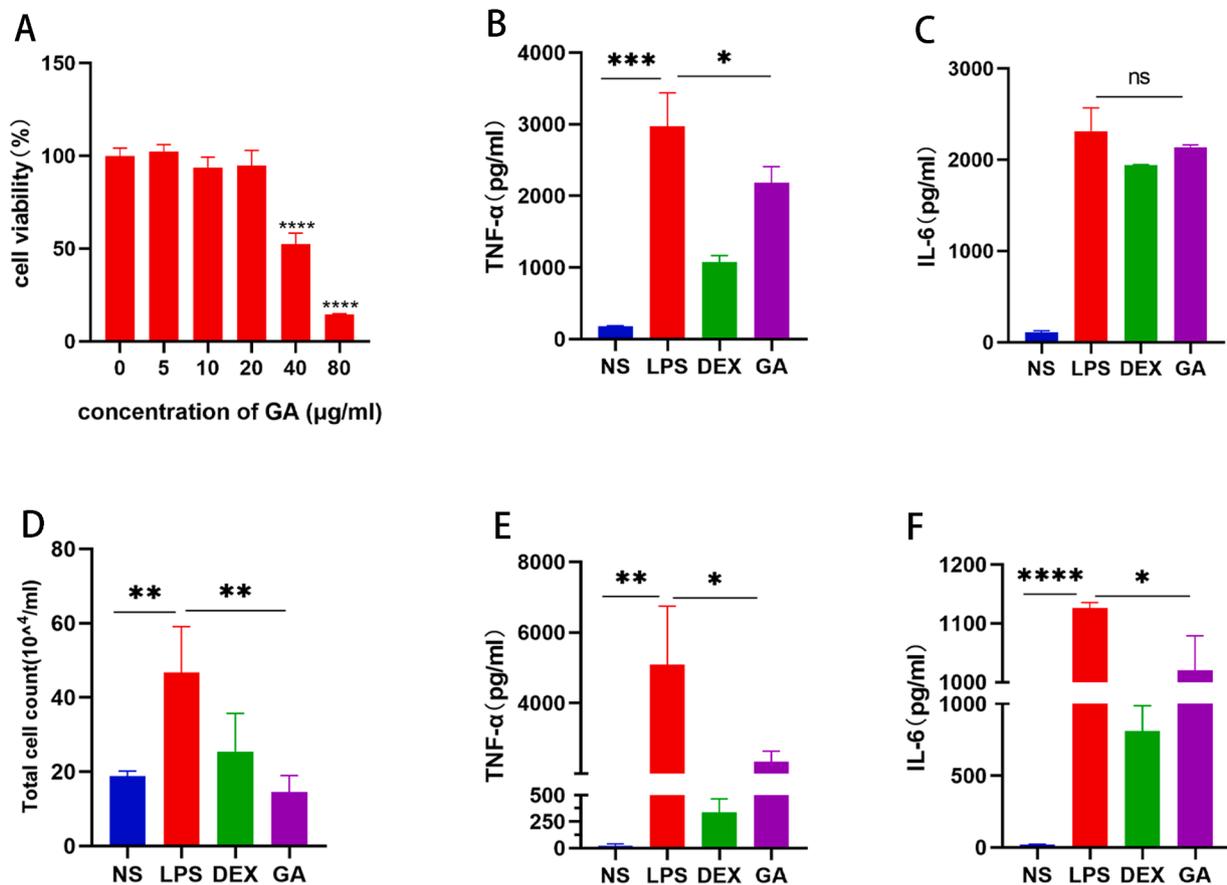
Fig. 6. The experimental results of GA inhibition of CS in an *in vitro* and *in vivo* studies. (A) Cell viability assay of MH-S cells. (B, C) GA inhibited TNF-α and IL-6 *in vitro*. (D) GA inhibited total cell count in mouse BALF. (E,F) GA inhibited TNF-α and IL-6 *in vivo*. $*p < 0.05$, $**p < 0.01$, $***p < 0.001$, $****p < 0.0001$, compared with the control group.
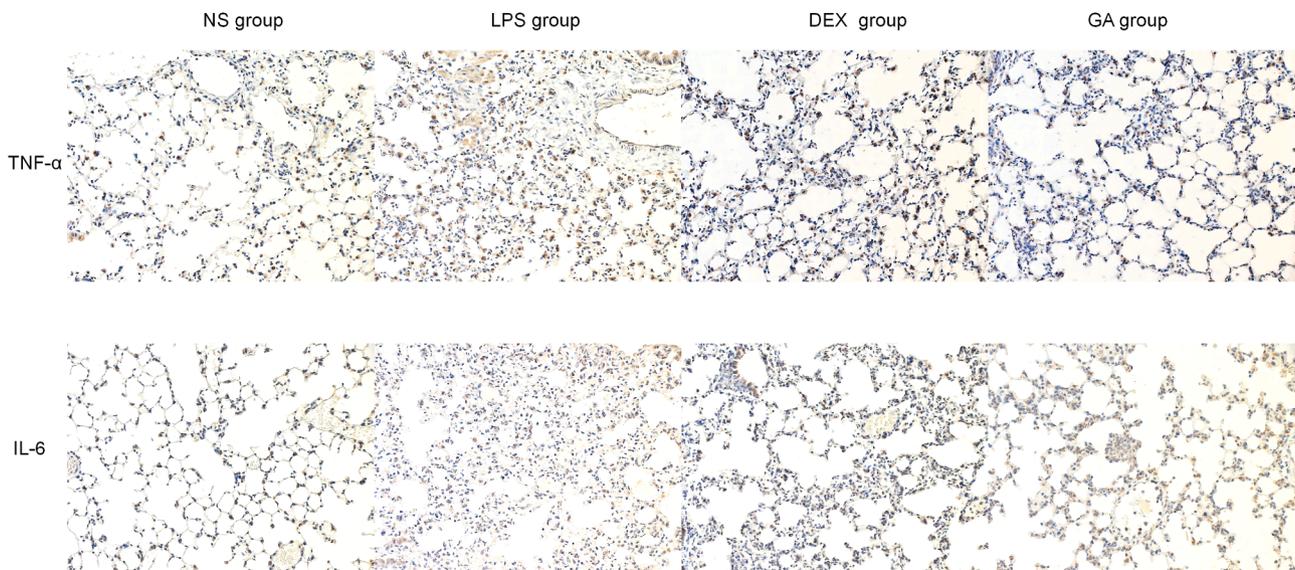
Fig. 7. Immunohistochemical results of TNF-α and IL-6 in lung tissue ($\times$ 200).

Meanwhile, a study showed that GA was cleared slowly in rats, and GA concentrations remained at high levels within 8 – 24 h after administration, and GA was also detectable in lung tissue, which is an important organ attacked by COVID-19 CS, suggesting a potential role for GA in CS (Yi et al., 2022).. And with the current successful application of biomaterials in the medical field, combining GA with suitable biomaterials may enable it to exert better anti-inflammatory effects (Yang et al., 2021). Moreover, the safety of licorice preparation is good, with no significant toxic side effects (Cinatl et al., 2003). Therefore, GA is a potentially effective and safe drug for the treatment of CS, which deserves further investigation.
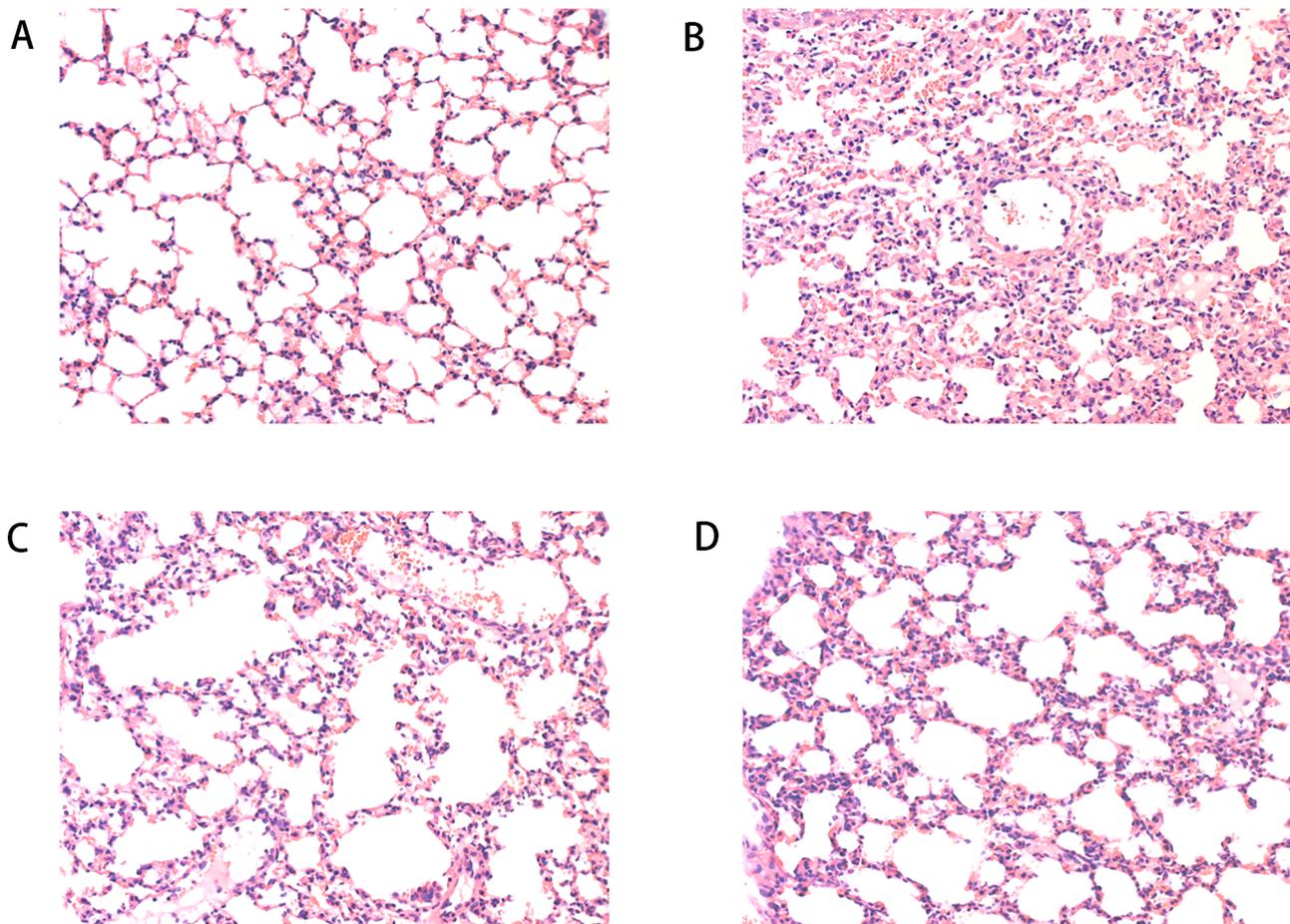
Fig. 8. The effects of GA on lung injury caused by LPS-induced CS ($\times$ 200). (A) NS group. (B) LPS group. (C) DEX group. (D) GA group.

Conclusion

In this research, we explored the underlying mechanism of GA for the treatment of CS through network pharmacology, molecular docking, and experimental verification. This study provides theoretically and practically basis for GA to be used as a promising drug for treating COVID-19 CS, which is worthy of further exploration.

Authors' contributions

Huawei Li, Jia You, Xi Yang, Yuanfeng Wei, Lingnan Zheng, Yaqin Zhao, Ying Huang, Zhao Jin, and Cheng Yi contributed to this work. Huawei Li, Jia You, and Xi Yang contributed equally to this work. Jin Zhao and Yi Cheng directed the design and implementation of this study. Huawei Li, Jia You, Xi Yang, Yuanfeng Wei and Lingnan Zheng participated in the specific experimental process and the writing of the paper. Yaqin Zhao and Ying Huang contributed to the production of the graphics. All authors have read and approved the final draft.

Funding

Declaration of Competing Interest

The authors state that there are no conflicts of interest.

Acknowledgments

References

Ahmad, S., Waheed, Y., Abro, A., Abbasi, S.W., Ismail, S., 2021. Molecular screening of glycyrrhizin-based inhibitors against ACE2 host receptor of SARS-CoV-2. J. Mol. Model. 27, 206.

Andreakos, E., Papadaki, M., Serhan, C.N., 2021. Dexamethasone, pro-resolving lipid mediators and resolution of inflammation in COVID-19. Allergy 76, 626–628.

Bailly, C., Vergoten, G., 2020. Glycyrrhizin: an alternative drug for the treatment of COVID-19 infection and the associated respiratory syndrome? Pharmacol. Ther. 214, 107618.

Behrens, E.M., Koretzky, G.A., 2017. Review: cytokine storm syndrome: looking toward the precision medicine era. Arthritis Rheumatol. 69, 1135–1143. Hoboken, N.J.

Blaser, H., Dostert, C., Mak, T.W., Brenner, D., 2016. TNF and ROS crosstalk in inflammation. Trends Cell Biol. 26, 249–261.

Chrzanowski, J., Chrzanowska, A., Graboń, W., 2021. Glycyrrhizin: An old weapon against a novel coronavirus. Phytother. Res. 35, 629–636.

Cinatl, J., Morgenstern, B., Bauer, G., Chandra, P., Rabenau, H., Doerr, H.W., 2003. Glycyrrhizin, an active component of liquorice roots, and replication of SARS-associated coronavirus. Lancet 361, 2045–2046. London, England.

Cron, R.Q., Caricchio, R., Chatham, W.W., 2021. Calming the cytokine storm in COVID-19. Nat. Med. 27, 1674–1675.

Dey, A., Sen, S., Maulik, U., 2021. Unveiling COVID-19-associated organ-specific cell types and cell-specific pathway cascade. Brief. Bioinform. 22, 914–923.

Ding, H., Deng, W., Ding, L., Ye, X., Yin, S., Huang, W., 2020. Glycyrrhetinic acid and its derivatives as potential alternative medicine to relieve symptoms in nonhospitalized COVID-19 patients. J. Med. Virol. 92, 2200–2204.

Fu, R., Li, J., Yu, H., Zhang, Y., Xu, Z., Martin, C., 2021. The yin and yang of traditional Chinese and western medicine. Med. Res. Rev. 41, 3182–3200.

Gao, Y., Xu, G., Wang, B., Liu, B., 2021. Cytokine storm syndrome in coronavirus disease 2019: a narrative review. J. Intern. Med. 289, 147–161.

Grimes, J.M., Grimes, K.V., 2020. p38 MAPK inhibition: a promising therapeutic approach for COVID-19. J. Mol. Cell Cardiol. 144, 63–65.

Guo, J., Shang, E., Zhao, J., Fan, X., Duan, J., Qian, D., Tao, W., Tang, Y., 2014. Data mining and frequency analysis for licorice as a "Two-Face" herb in Chinese formulae based on Chinese formulae database. Phytomedicine 21, 1281–1286.

He, T., Qu, R., Qin, C., Wang, Z., Zhang, Y., Shao, X., Lu, T., 2020. Potential mechanisms of Chinese herbal medicine that implicated in the treatment of COVID-19 related renal injury. Saudi Pharm. J. 28, 1138–1148. SPJ: the official publication of the Saudi Pharmaceutical Society.

Horby, P., Lim, W.S., Emberson, J.R., Mafham, M., Bell, J.L., Linsell, L., Staplin, N., Brightling, C., Ustianowski, A., Elmahi, E., Prudon, B., Green, C., Felton, T., Chadwick, D., Rege, K., Fegan, C., Chappell, L.C., Faust, S.N., Jaki, T., Jeffery, K., Montgomery, A., Rowan, K., Juszczak, E., Baillie, J.K., Haynes, R., Landray, M.J., 2021. Dexamethasone in hospitalized patients with Covid-19. N. Engl. J. Med. 384, 693–704.

Hu, K., Guan, W., Bi, Y., Zhang, W., Li, L., Zhang, B., Liu, Q., Song, Y., Li, X., Duan, Z., Zheng, Q., Yang, Z., Liang, J., Han, M., Ruan, L., Wu, C., Zhang, Y., Jia, Z., Zhong, N., 2021. Efficacy and safety of Lianhuaqingwen capsules, a repurposed Chinese herb, in patients with coronavirus disease 2019: a multicenter, prospective, randomized controlled trial. Phytomedicine 85, 153242.

Kalliolias, G.D., Ivashkiv, L.B., 2016. TNF biology, pathogenic mechanisms and emerging therapeutic strategies. Nat. Rev. Rheumatol. 12, 49–62.

Kawai, T., Akira, S., 2006. Innate immune recognition of viral infection. Nat. Immunol. 7, 131–137.

Kim, J.S., Lee, J.Y., Yang, J.W., Lee, K.H., Effenberger, M., Szpirt, W., Kronbichler, A., Shin, J.I., 2021. Immunopathogenesis and treatment of cytokine storm in COVID-19. Theranostics 11, 316–329.

Kovalchuk, A., Wang, B., Li, D., Rodriguez-Juarez, R., Ilnytskyy, S., Kovalchuk, I., Kovalchuk, O., 2021. Fighting the storm: could novel anti-TNFα and anti-IL-6 C. Sativa cultivars tame cytokine storm in COVID-19? Aging 13, 1571–1590.

Li, Y., Li, B., Wang, P., Wang, Q., 2021. Traditional Chinese medicine, qingfei paidu decoction and xuanfei baidu decoction, inhibited cytokine production via NF-κB Signaling pathway in macrophages: implications for coronavirus disease 2019 (COVID-19) therapy. Front. Pharmacol. 12, 722126.

Lin, H., Wang, X., Wang, L., Dong, H., Huang, P., Cai, Q., Mo, Y., Huang, F., Jiang, Z., 2019. Identified the synergistic mechanism of drynariae rhizoma for treating fracture based on network pharmacology. Evid. Based Complement. Altern. Med. 2019, 7342635 eCAM.

Oray, M., Abu Samra, K., Ebrahimiadib, N., Meese, H., Foster, C.S., 2016. Long-term side effects of glucocorticoids. Expert Opin. Drug Saf. 15, 457–465.

Pedersen, S.F., Ho, Y., 2020. SARS-CoV-2: a storm is raging. J. Clin. Invest. 130, 2202–2205.

Pooladanda, V., Thatikonda, S., Muvvala, S.P., Devabattula, G., Godugu, C., 2021. BRD4 targeting nanotherapy prevents lipopolysaccharide induced acute respiratory distress syndrome. Int. J. Pharmaceut. 601, 120536.

Qiao, L., Huang, W., Zhang, X., Guo, H., Wang, D., Feng, Q., Jin, R., Xie, L., Li, W., Cheng, J., 2021. Evaluation of the immunomodulatory effects of anti-COVID-19 TCM formulae by multiple virus-related pathways. Signal Transduct. Target. Ther. 6, 50.

Saghazadeh, A., Rezaei, N., 2020. Immune-epidemiological parameters of the novel coronavirus - a perspective. Expert Rev. Clin. Immunol. 16, 465–470.

Shawky, E., Nada, A.A., Ibrahim, R.S., 2020. Potential role of medicinal plants and their constituents in the mitigation of SARS-CoV-2: identifying related therapeutic targets using network pharmacology and molecular docking analyses. RSC Adv. 10, 27961–27983.

Shibabaw, T., 2020. Inflammatory cytokine: IL-17A signaling pathway in patients present with COVID-19 and current treatment strategy. J. Inflamm. Res. 13, 673–680.

Sun, Z., He, G., Huang, N., Thilakavathy, K., Lim, J.C.W., Kumar, S.S., Xiong, C., 2021. Glycyrrhizic acid: a natural plant ingredient as a drug candidate to treat COVID-19. Front. Pharmacol. 12, 707205.

Tanaka, T., Narazaki, M., Kishimoto, T., 2016. Immunotherapeutic implications of IL-6 blockade for cytokine storm. Immunotherapy 8, 959–970. -Uk.

Thomas, G., Frederick, E., Thompson, L., Bar-Or, R., Mulugeta, Y., Hausburg, M., Roshon, M., Mains, C., Bar-Or, D., 2020. LMWF5A suppresses cytokine release by modulating select inflammatory transcription factor activity in stimulated PBMC. J. Transl. Med. 18, 452.

Vallée, A., Lecarpentier, Y., Vallée, J., 2021. Interplay of opposing effects of the WNT/β-catenin pathway and PPARγ and implications for SARS-CoV2 treatment. Front. Immunol. 12, 666693.

Wei, P., 2020. Diagnosis and treatment protocol for novel coronavirus pneumonia (Trial Version 7). Chin. Med. J. Peking 133, 1087–1095.

Wu, Y., Yeh, I., Phan, N.N., Yen, M., Liu, H., Wang, C., Hsu, H., 2021. Severe acute respiratory syndrome coronavirus (SARS-CoV)-2 infection induces dysregulation of immunity: in silico gene expression analysis. Int. J. Med. Sci. 18, 1143–1152.

Yang, S., Wu, S., Yu, Z., Huang, J., Zhong, X., Liu, X., Zhu, H., Xiao, L., Deng, Q., Sun, W., 2020. Transcriptomic analysis reveals novel mechanisms of SARS-CoV-2 infection in human lung cells. Immun.Inflamm. Dis. 8, 753–762.

Yang, X., You, J., Wei, Y., Li, H., Gao, L., Guo, Q., Huang, Y., Gong, C., Yi, C., 2021. Emerging nanomaterials applied for tackling the COVID-19 cytokine storm. J. Mater. Chem. B 9, 8185–8201.

Yi, Y., Li, J., Lai, X., Zhang, M., Kuang, Y., Bao, Y., Yu, R., Hong, W., Muturi, E., Xue, H., Wei, H., Li, T., Zhuang, H., Qiao, X., Xiang, K., Yang, H., Ye, M., 2022. Natural triterpenoids from licorice potently inhibit SARS-CoV-2 infection. J. Adv. Res. 36, 201–210.

Yongzhi, X., 2021. COVID-19-associated cytokine storm syndrome and diagnostic principles: an old and new Issue. Emerg. Microbes Infect. 10, 266–276.

Yu, S., Zhu, Y., Xu, J., Yao, G., Zhang, P., Wang, M., Zhao, Y., Lin, G., Chen, H., Chen, L., Zhang, J., 2021. Glycyrrhizic acid exerts inhibitory activity against the spike protein of SARS-CoV-2. Phytomedicine 85, 153364 international journal of phytotherapy and phytopharmacology.

Zhao, H., Zhao, M., Wang, Y., Li, F., Zhang, Z., 2016. Glycyrrhizic acid prevents sepsis-induced acute lung injury and mortality in rats. The journal of histochemistry and cytochemistry: official J. Histochem. Soc. 64, 125–137.

Zígolo, M.A., Goytia, M.R., Poma, H.R., Rajal, V.B., Irazusta, V.P., 2021. Virtual screening of plant-derived compounds against SARS-CoV-2 viral proteins using computational tools. Sci. Total Environ. 781, 146400.